

## Effects of 0.5wt% In on Precipitation Processes in Al-Cu-(Li) Alloys

Zhengrong Pan, Ziqiao Zheng, Shichen Li, Zhongquan Liao

(School of Materials Science and Engineering, Central South University, Changsha 410083, China)

Precipitation on and along both the  $\langle 001 \rangle_{\alpha}$  and the  $\{001\}_{\alpha}$  crystal systems by microalloying Al-3.5Cu-(1.0Li) base alloy with 0.5wt.% Indium were produced. Using differential scanning calorimetry, transmission electron microscopy and three-dimensional atom probe, we have demonstrated that In addition effects varies with the base alloy: addition of Indium markedly accelerated the aging process of Al-Cu alloy at 175°C, and raise the peak hardness of the alloy about 20HV. In-rich particles precipitate distributed at the early stage of aging, which would then act as heterogeneous nucleation positions of  $\theta'$  phase; In' particles were observed at one corner of platelets having their broad face in the plane of view;  $\theta$  phase coarse ned much slower in In-added alloy than In-free alloy. A cubic phase, which has not been previously reported in In-free alloy with such composition, emerged in Al-Cu-Li-In alloy dispersively. Indium could aid the nucleation of cubic phase by arresting vacancies from forming dislocation loops, reducing the number of heterogeneous sites available for  $T_1$  nucleation by slowing down nucleation of the equilibrium  $T_1$  phase.

**Key words:** Indium, microalloying, precipitation, cubic phase, Al-Cu-(Li) alloys

### 1. Introduction

Trace addition of In to Al-Cu system stimulate the heterogeneous nucleation of  $\theta'$  precipitates, improve significantly the age hardening response<sup>[1]</sup>. Numerous studies have been undertaken to understand the nature and mechanism of this microstructural refinement. Silcock<sup>[2]</sup> have proposed that the nucleation mechanism depends on aging temperature and that heterogeneous precipitation on In precipitates at higher temperatures ( $\geq 200^{\circ}\text{C}$ ) and that at lower temperatures, nucleation involves directly the In-V clusters and their incorporation into the  $\theta'$  structure. In contrast, much less work has been done on Indium microalloyed Al-Cu-Li system. Gilmore<sup>[3]</sup> thought Indium effects precipitation in two ways: by increasing the thickness of the  $\{111\}$  plates during the early stages of ageing and later by promoting more homogeneous precipitation of  $T_1$  in the matrix. Several other authors<sup>[4]</sup> have concluded that In precipitates out of the matrix as fine spherical particles during the early stages of aging. These particles would then act as heterogeneous nucleation sites for the  $\theta'$  or  $T_1$  phase.

### 2. Experimental procedure

Alloys were prepared from elemental components of high purity (>99.9%). The ingots obtained were homogenized, hot-and-cold rolled to 1.8mm sheet. The samples were solution treated at 530°C for 1 hour followed by immediate quenching into cold water and then aged at 175°C(T6) or at 155°C after 6% pre-deformation(T8). Hardness measurement was carried on MTK1000A, with 1.96N loading 15s. Discs of 3 mm diameter were electro-polished using a solution of 25% nitric acid and 75% methanol, for TEM (HREM) operation. The microstructures were examined in Tecnai G<sup>2</sup>20 TEM and Tecnai G<sup>2</sup> F30 Field Emission TEM operating at 200kv, 300kv, respectively. 3DAP sample was tested in an environment in-chamber vacuum  $<10^{-10}$  mbar, -25 °C; data obtained were analyzed by the expert system PoSAP. Chemical compositions of studied alloys were listed in Table 1.

### 3. Results and discussion

Age hardening responses at 175°C of studied alloys were shown in Figure 1. Alloy A1 took some 25h to achieve the maximum hardness, in alloy A2 the time to maximum hardness was reduced to 7h, and the level of maximum hardness increased significantly (Figure 1a). The addition of Indium brought a similar increment of maximum hardness to B2, while B1/B2 both took about 60h to the hardness peak.

Table 1. Chemical compositions wt.%

Alloy	Cu	Li	In	Zr	Al
A1	3.39	-	-	0.12	Bal
A2	3.29	-	0.45	0.12	Bal
B1	3.2	0.7	-	0.12	Bal
B2	3.28	0.76	0.44	0.12	Bal

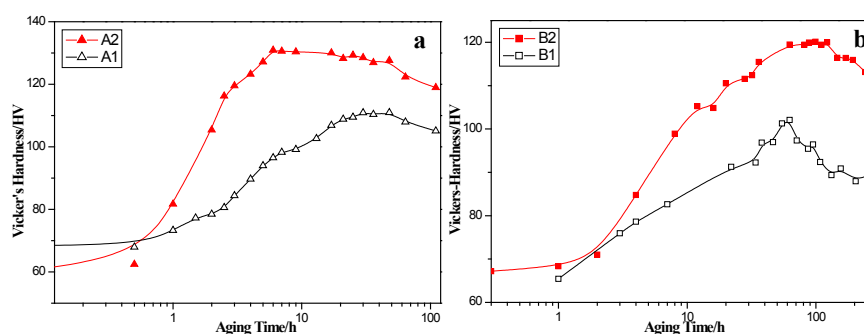


Fig. 1. Hardness-Time curves for studied alloys aging at 175°C  
(a)Al-Cu-(In); (b)Al-Cu-Li-(In)

### 3.1 Al-Cu-(In)

The sequences of precipitation in Al-Cu-(In) alloys at 175°C and peak aged tomography in T8 condition were provided in Fig. 2. The micrographs were recorded near the  $\langle 001 \rangle_\alpha$  orientation and provided an overview of the general microstructure together with the relevant typical  $\langle 001 \rangle_\alpha$  SAED patterns. The inserted SAED in Figure 2a<sub>1</sub> exhibits continuous diffuse streaks toward the  $\langle 001 \rangle_\alpha$  direction, indicating the presence of GP. zones in under-aged (2h) alloy A1; when peak aged 25h, the  $\langle 001 \rangle_\alpha$  streaks contain weak intensity maximum in Figure 2a<sub>2</sub>, reveals that GP. zones has transformed into  $\theta''$  phase<sup>[5]</sup>; over-aged(60h) SAED observes typical  $\theta'$  pattern. In contrast, the diffraction patterns of the In-added alloy aged for 2h to 200h shows the exhibiting of  $\theta'$  precipitates. Details of 175°C aged alloy A2 were presented in Fig. 2c. Small dark spots (see arrows) were observed at one corner of many platelets having their broad face in the plan of view throughout the process and becoming clear. According to Kanno<sup>[6]</sup> and Bourgeois<sup>[7]</sup>, these dark spots were In-rich particles, which would then act as heterogeneous nucleation positions of  $\theta$  phase. Both the SAEDs and BF images gave out that:  $\theta'$  phase precipitates earlier and coarsen much slower in In-added A2 than In-free A1 alloy. After 6% pre-deformation, dark In-rich particles no longer exist; this may suggest that in T6 state Indium facilitating  $\theta'$  mainly through quenched-in vacancies.

### 3.2 Al-Cu-Li-(In)

The sequence of precipitation in the Al-Cu-Li-(In) alloy aged at 175°C is provided in Fig. 3. The under-aged ternary image shows the formation of dislocation loops and helices (Fig. 3a<sub>1</sub>). In contrast, dislocation were generally absent from the microstructure of the In-containing B2 alloy (Fig.3a<sub>2</sub>). The BF image (Fig. 3a<sub>3</sub>) recorded from the specimen aged for 4h reveals just faint contrast of twin lobe as arrowed, no clear diffraction associated with other decompositions were observed in the corresponding SAED. Alloy B1 uniformly precipitate T<sub>1</sub> phase (Fig. 3b<sub>1</sub>), dispersed  $\theta'$  plate. Fine and uniform dispersion  $\theta'$  platelets, large quantities of square shaped phase were observed in peak aged

B2 alloy (Fig. 3b<sub>2</sub> and b<sub>3</sub>), which will be referred to as  $\chi$  throughout this paper for simplicity. Also observed at this aging temperature were T<sub>1</sub> phase precipitates, contrast from this phase is available by exhibiting thickness-fringes inclined to the electron beam (arrowed in Fig. 3b<sub>2</sub> and b<sub>3</sub>). Unlike previous reported Indium promoting more homo-or-heterogeneous precipitation of T<sub>1</sub> in the matrix of Al-Cu-Li alloy, there was no dark In-rich particles observed and the density of T<sub>1</sub> phase is quite lower than B1 alloy (Fig. 1b).

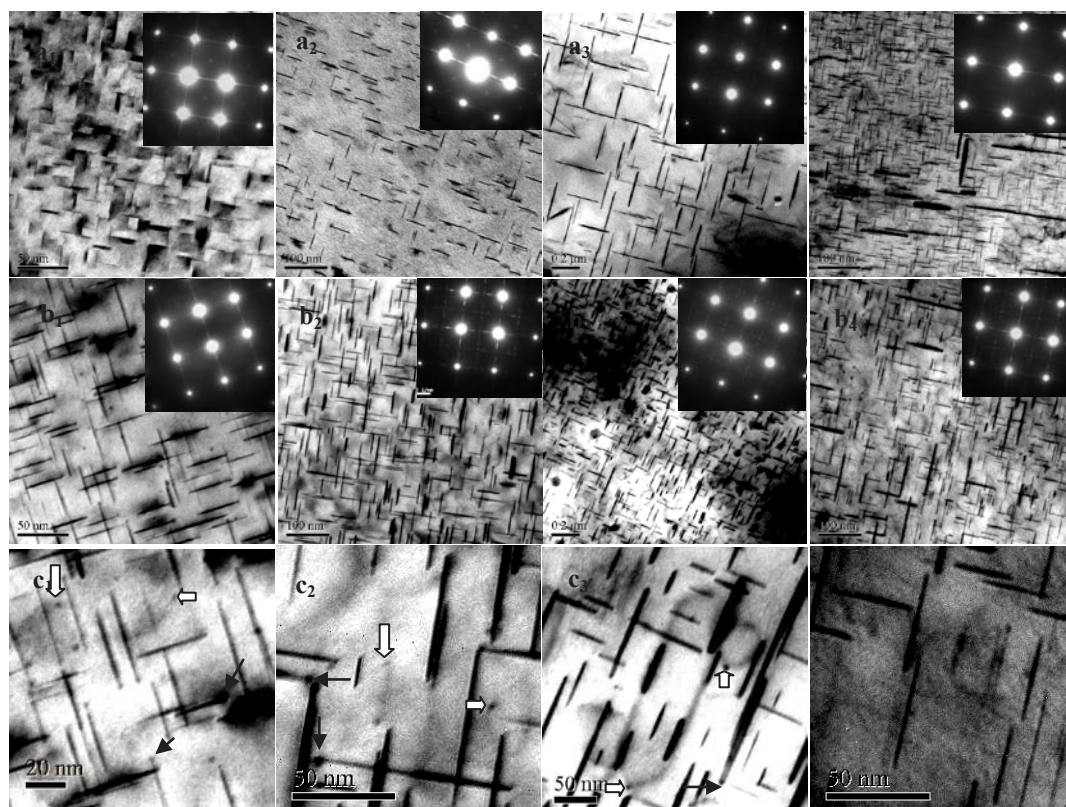


Fig. 2. Electron micrographs with diffraction patterns close to the  $\langle 001 \rangle_{\alpha}$   
 T6 Under aged (a<sub>1</sub>) Al-Cu/2h; (b<sub>1</sub>), (c<sub>1</sub>)Al-Cu-In/2h  
 T6 Peak aged (a<sub>2</sub>) Al-Cu/24h; (b<sub>2</sub>), (c<sub>2</sub>)Al-Cu-In/7h  
 T6 Over aged (a<sub>3</sub>) Al-Cu/60h; (b<sub>3</sub>), (c<sub>3</sub>)Al-Cu-In/120h  
 T8 Peak aged (a<sub>4</sub>) Al-Cu/24h; (b<sub>4</sub>), (c<sub>4</sub>)Al-Cu-In/24h

6% pre-deformation made a reduction in precipitate size and increased homogeneity of the  $\theta'$  distribution to both alloys, but the cubic phase was no longer visible in Al-Cu-Li-In alloy. Fig. 3c represents the microstructure and corresponding SAED pattern along  $\langle 001 \rangle_{\alpha}$  direction, showing large quantity of T<sub>1</sub> phase, confirmed by the  $\langle 112 \rangle_{\alpha}$  direction (Fig. 3c<sub>2</sub>). It seems that  $\chi$  phase and T<sub>1</sub> phase is either dominant or less, clearly proving their competition precipitation. This view is supported by the observation that a pre-age deformation substantially increases the volume fraction of T<sub>1</sub> at the expense of  $\chi$  phase. In fact, the cubic  $\chi$  phase forming in Al-Cu-Li alloy was also detected in Fig. 3b<sub>1</sub> (arrowed as 1).

Phenomenologically, it would be seen that the presence of Indium is required for the nucleation of this  $\chi$  precipitate. In fact, Fig. 4 provided 3DAP elemental maps of peak aged alloy B2 at 175°C, it reveals that there are numbers of cubic Cu-cluster, while Indium atoms distribute uniformly. The scanning transmission electron microscopy EDXS analysis in Fig. 5 revealed that In was not detected in association with the cubic precipitate, thereby indicating that Indium atoms or clusters can not provide nucleation sites for  $\chi$ .

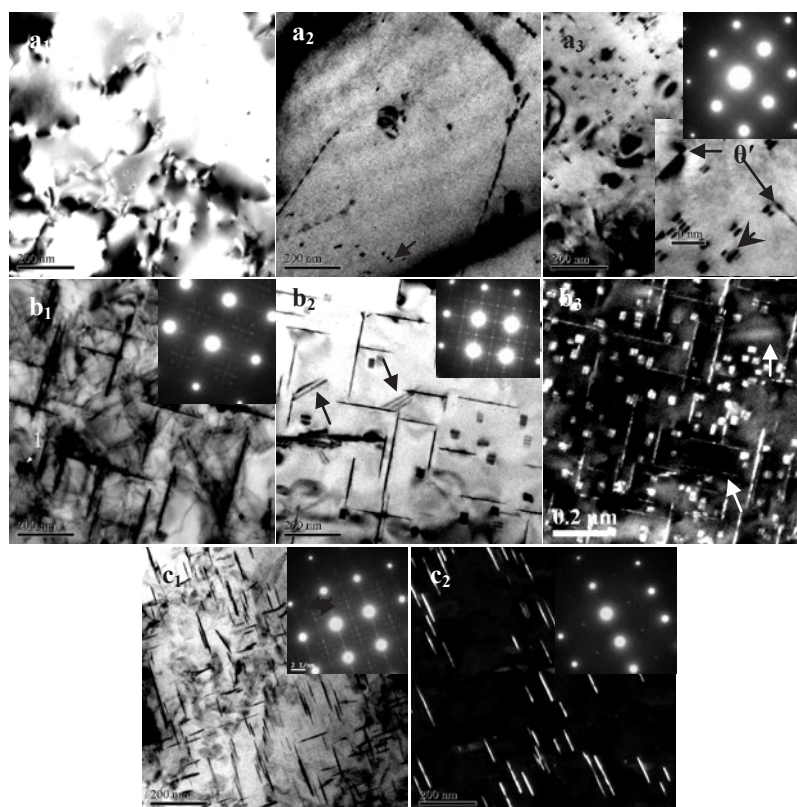


Fig. 3. Electron micrographs with diffraction patterns  
 T6 Under aged (a<sub>1</sub>) Al-Cu-Li/2h; (a<sub>2</sub>) Al-Cu-Li-In/2h; (a<sub>3</sub>) Al-Cu-Li-In/4h  
 T6 Peak aged (b<sub>1</sub>) Al-Cu-Li/50h; (b<sub>2</sub>) Al-Cu-Li-In/40h,BF; (b<sub>3</sub>) Al-Cu-Li-In/40h,DF  
 T8 Peak aged Al-Cu-Li-In/36h (c<sub>1</sub>) B=[100]<sub>a</sub>; (c<sub>2</sub>) B=[112]<sub>a</sub>

But it might aid the nucleation of this phase by slowing down nucleation of the equilibrium T<sub>1</sub> phase. Shapes of precipitates vary as the competition of surface energy and volume strain energy. A new phase precipitates from the matrix as plates or needles instead of spherical. Surface energy is just determined by the specific surface area if specific surface energy is given, clearly, spherical precipitates have the smallest specific surface area. To minimize surface energy the precipitate could be spheres but not plates or needles. From shapes of studied T<sub>1</sub> and  $\chi$  phases, it could be known that T<sub>1</sub> phase has a much greater strain energy than surface free energy; while  $\chi$  opposites.

When nucleated on dislocations, in addition to the usual volume and surface energy terms in the expression for the energy of formation of a nucleus of given size, there is a term representing the strain energy of the dislocation in the region now occupied by the new phase. In effect, the atomic rearrangement within the nucleus is assumed to destroy that part of the elastic energy of the dislocation located in the volume of the nucleus, and the energy thus gained is available to help the nucleation process.

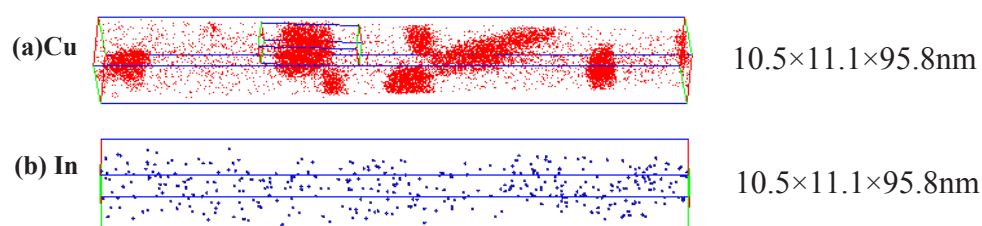


Fig 4. 3DAP elemental maps of peak aged Al-Cu-Li-In alloy for (a)Cu and (b) In

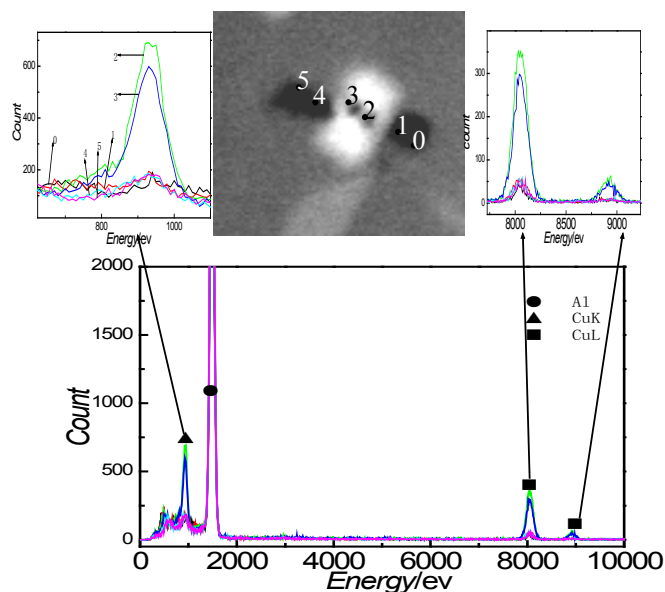


Fig. 5. STEM micrograph of a cubic phase close to  $\langle 001 \rangle_a$ , EDXS spectra, inseting enlargements of Cu regions.

Thus a precipitate having a relative large strain energy nucleation would be much sensitive to the dislocations:  $T_1$  phase nucleation will be greatly accelerated by dislocations, and much less effect would happen to the cubic  $\chi$  phase. Indium has the strongest bond to vacancies. It was certificated that with the addition of Indium, vacancy loops no longer formed in the alloy (Fig. 3a<sub>2</sub>).

#### 4. Conclusions

1. In Al-Cu-In alloy, In-rich particles precipitate distributedly at the early stage of aging, which would then act as heterogeneous nucleation positions of  $\theta'$  phase; In particles were observed at one corner of platelets having their broad face in the plane of view.
2. The addition of 0.5wt% Indium in this alloy radically affected the microstructure evolution, inhibiting the formation of  $T_1$  by promotion of a cubic  $\chi$  phase.
3. The nucleation of  $\chi$  phase appears to be homogenous, and it's formation is competitive with  $T_1$  phase. Indium could aid the nucleation of  $\chi$  phase by arresting vacancies from forming dislocation loops, reducing the number of heterogeneous sites available for  $T_1$  nucleation by slowing down nucleation of the equilibrium  $T_1$  phase.

#### Acknowledgments

The authors thank the National Natural Science Foundation 2009 of China (No. 50801067) for financial support.

#### References

- [1] H. K. Hardy: *Journal of the Institute of Metals*. 78 (1950-51) 169.
- [2] J. M. Silcock, H. M. Flower: *Scripta Materialia*. 46 (2002) 389-394.
- [3] D. L. Gilmore, E. A. Starke: *Metallurgical and Materials Transactions A*. 28 (1997) 1399-1415
- [4] A. K. Mukhopadhyay, K. S. Prasad, C. R. Chakravorty: *Materials Science Forum*. 217-222 (1996) 753-758.
- [5] J. L. Murray: *International metals reviews*. 30 (1985) 211-233.
- [6] M. Kanno, H. Suzuki, O. Kanoh: *Journal of Japanese Institute of Metals*. 44 (1980) 1139-1145.
- [7] L. Bourgeois, J. F. Nie, B. C. Muddle: *Philosophical Magazine*. 85 (2005) 3487-3509.